

Photooxidation of cyclohexane and cyclohexene in BaY

G. Li, M. Xu, S.C. Larsen*, V.H. Grassian

Department of Chemistry, University of Iowa, Iowa City, IA 52242 USA

Received 18 June 2002; received in revised form 20 August 2002; accepted 20 August 2002

Abstract

In this study, in situ FT-IR spectroscopy and ex situ GC and GC-MS were employed to investigate the photooxidation of cyclohexane and cyclohexene in BaY. Cyclohexane and cyclohexene were oxidized using molecular oxygen and photochemically produced *tert*-butyl hydroperoxide (TBHP) in BaY. The main products formed after photooxidation of cyclohexane with molecular oxygen were cyclohexanone and cyclohexanol. Cyclohexane did not react with TBHP in BaY. The main product formed after photooxidation of cyclohexene and molecular oxygen in BaY was 2-cyclohexen-1-one and the main product formed after reaction of cyclohexene with TBHP in BaY was 1,2-epoxy cyclohexane. In general, it was found that the photooxidation of cyclohexene using O₂ or TBHP gave consistently higher activity but lower selectivity than that found for cyclohexane photooxidation, due to the presence of two active reaction centers (α -H and C=C bond) in cyclohexene. It was also shown that for cyclohexene oxidation in BaY, the choice of oxidant significantly alters the product distribution.

© 2002 Elsevier Science B.V. All rights reserved.

Keywords: Photooxidation; Y zeolite; Cyclohexane; Cyclohexene; TBHP

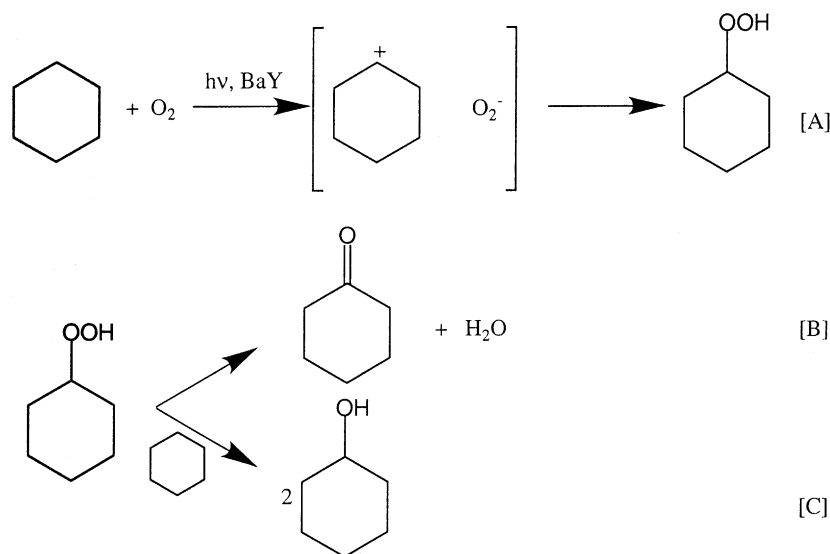
1. Introduction

Catalyzed partial oxidation of small hydrocarbons using molecular oxygen has been a very important process used to obtain industrially important chemicals. The products serve as building blocks for plastics and synthetic fibers, or as industrial intermediates in the manufacture of fine chemicals [1–4]. Typically, direct oxidation of small hydrocarbons by O₂ gives very poor selectivity due to the free radical nature of the process, the high exothermicity of the reactions and/or overoxidation [5]. The accumulation of by-products also limits conversion to a few percent

in most practical processes. The inefficiency associated with low conversion has motivated the search for solid catalysts that are active for the oxidation of hydrocarbons [6–12]. Ramamurthy and co-workers have studied singlet oxygen mediated selective oxidation reactions in dye-exchanged Y zeolites [13]. Transition-metal substituted molecular sieves have also been shown to be active for selective oxidation reactions in air [6–8,10,14].

Recently, Frei and co-workers [1,12,15–24] and Larsen, Grassian and co-workers [4,25–30] have explored the use of cation-exchanged zeolites in the room temperature selective photo- and thermal oxidation of olefins, alkyl-substituted benzenes, and alkanes. The oxidation is initiated by excitation of a hydrocarbon oxygen complex occluded in the zeolite to form a low-energy charge transfer state that is stabilized by the electric field at the cation site in the zeolite [15,23]. The high selectivity of these

* Corresponding author. Tel.: +1-319-335-1346 (S.C. Larsen)/+1-319-335-1392 (V.H. Grassian); fax: +1-319-335-1270 (S.C. Larsen and V.H. Grassian).
E-mail addresses: sarah-larsen@uiowa.edu (S.C. Larsen), vicki-grassian@uiowa.edu (V.H. Grassian).



Scheme 1. Proposed mechanism for the photooxidation of cyclohexane with O_2 in BaY.

reactions can be attributed to several factors. First, using low reaction temperatures inhibits some free radical chemistry. Second, the use of visible light rather than UV light provides a low-energy pathway and third, the zeolite cavity results in a caging effect.

In a previous study, we investigated the kinetics of the photo- and thermal reactions of cyclohexane in BaY [30]. The proposed reaction mechanism for this reaction is shown in Scheme 1 [12]. Using visible light or mild thermal conditions, oxidation of cyclohexane in BaY with molecular oxygen produces cyclohexanone and cyclohexanol. The activation energy was measured for the thermal process and it was consistent with a mechanism that proceeded through a charge-transfer complex. Based on kinetic isotope effect studies, the rate-determining step was assigned to the proton abstraction step in Scheme 1A. Since the kinetic isotope effects were the same for the thermal and photochemical processes, the mechanism was proposed to be the same for both reactions.

In this study, the photooxidation of cyclohexane and cyclohexene in BaY zeolite using in situ FT-IR, and ex situ GC and GC-MS was examined. A direct comparison of the photooxidation of cyclohexane versus cyclohexene in BaY using molecular oxygen and tertiary butyl hydroperoxide (TBHP) was made in order to elucidate the factors that influence product selectiv-

ity in these reactions. These factors include the excitation wavelength, the reactant and the oxidant.

2. Experimental

2.1. Zeolite sample preparation

BaY was prepared from NaY (Aldrich) by standard ion-exchange procedures. NaY was added to an aqueous 0.5 M $BaCl_2$ solution and heated to 90 °C for 24 h. The resulting solution was filtered and the zeolite was washed with deionized water until the solution was free of Cl^- ions as determined by adding $AgNO_3(aq)$ to the filtrate solution until no precipitate was observed. The elemental composition of Al, Si and Ba was determined by inductively coupled plasma/atomic emission spectroscopy (ICP/AES) using a Perkin-Elmer Plasma 400. The Si/Al and Ba/Al ratios for BaY were 2.4 and 0.33, respectively. BaY was activated by heating overnight to 300 °C under vacuum.

2.2. FT-IR spectroscopy

The infrared sample cell used in this study is shown in Fig. 1. Approximate 50 mg BaY zeolite was coated

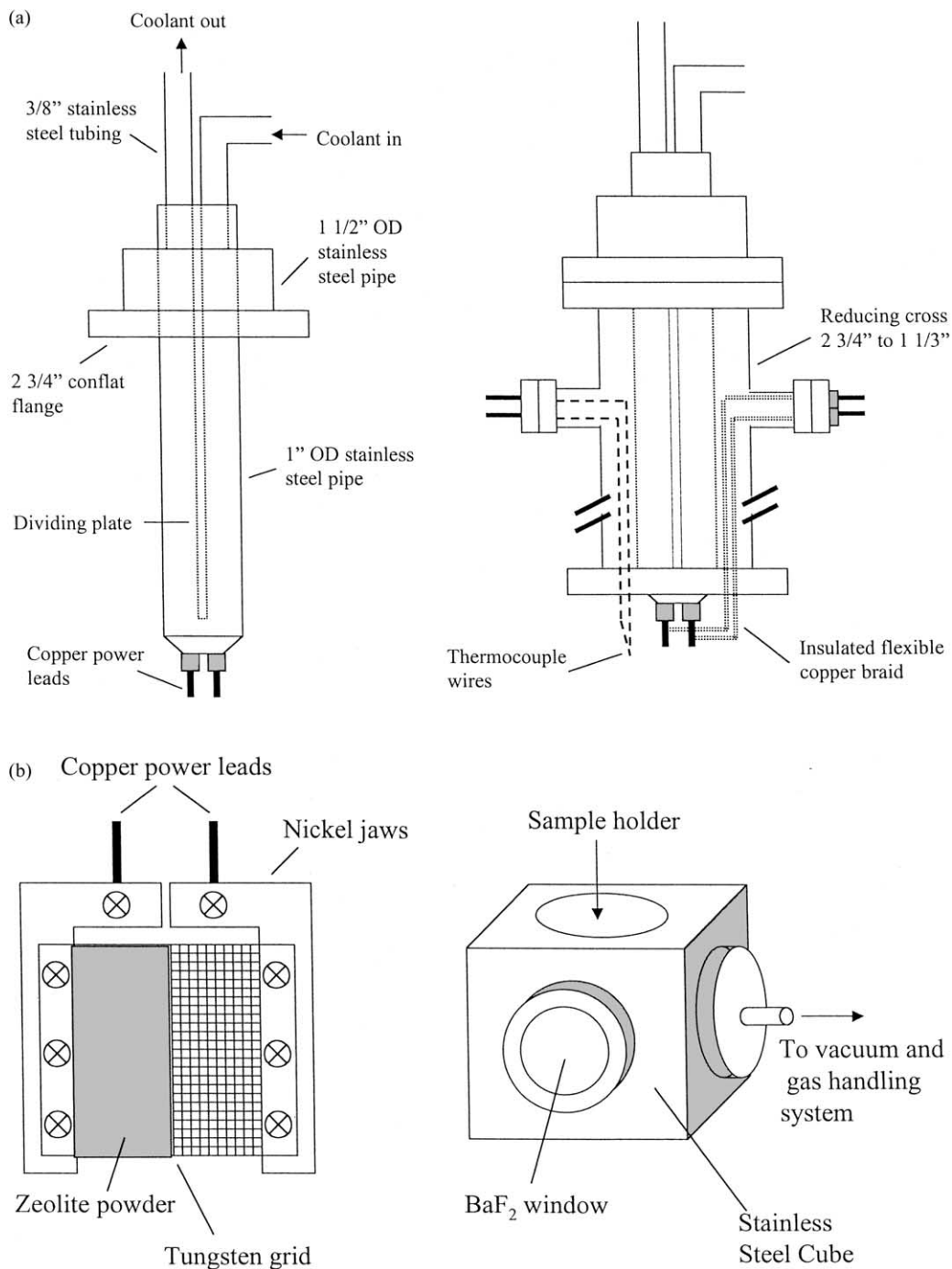


Fig. 1. Schematic of the infrared sample cell used to study photooxidation reactions in zeolites. (a) A stainless steel coolant system (left) with copper power leads welded to the end of a stainless steel pipe is put inside of a stainless steel reducing cross (right). (b) The copper power leads shown in (a) are attached to copper power leads that are connected to nickel jaws so that the tungsten grid held in place by the nickel jaws (left) could be resistively heated. Thermocouple wires shown in (a) are spot-welded to the tungsten grid to measure the temperature. After attaching the nickel jaw assembly (left) to (a) the entire reducing cross is then placed in a stainless steel cube. The cube has two BaF₂ windows to transmit infrared radiation and can be attached to a vacuum/gas handling system.

onto a 3 cm × 2 cm photoetched tungsten grid held in place by nickel jaws. The nickel jaws are attached to copper leads so that the sample can be resistively heated. A thermocouple wire is used to measure the temperature of the sample. The tungsten grid with zeolite sample is placed in a stainless steel cube. The cube is outfitted with two BaF₂ windows for infrared measurements (vide infra) and is also attached to a vacuum/gas handling system [31]. The BaY sample was heated under vacuum to 300 °C overnight to remove adsorbed water. For in situ experiments using FT-IR spectroscopy, FT-IR spectra were recorded with a Mattson Galaxy 6000 infrared spectrometer equipped with a narrowband MCT detector. Each spectrum was obtained by averaging 500 scans at an instrument resolution of 4 cm⁻¹.

In oxidation experiments using molecular oxygen, cyclohexane or cyclohexene was loaded into the zeolite by adsorption at different hydrocarbon gas pressures that corresponded to different hydrocarbon loadings as described in detail in Section 3. The excess hydrocarbon was then pumped out, and oxygen was added to the IR cell at a pressure of 750 Torr. A 500-W mercury arc lamp (Oriol Corp) with a water filter was used as the light source. Broadband long pass filters were placed in front of the lamp. The broadband light was turned by a quartz prism onto the zeolite sample. The quartz prism is mounted inside the FT-IR sample compartment so that the dry air purge was not broken during irradiation. A schematic of the optical set-up is shown in Fig. 2.

In oxidation experiments using TBHP, TBHP was obtained by photooxidation of isobutane using molecular oxygen at a temperature of 273 K [21]. The excess isobutane and oxygen were then pumped out, and cyclohexane or cyclohexene was added to the IR cell at room temperature for oxidation in the dark.

2.3. GC analysis

Products were extracted from the zeolite in acetonitrile for 90 min before GC or GC–MS analysis. The sample was centrifuged for 2 min at 10,000 × g and the supernatant was then analyzed by GC or GC–MS. The GC (Varian 3600) was equipped with an FID detector and a 5% phenyl/95% methylpolysiloxane capillary column. In some experiments GC–MS analysis was conducted, using a GC–MS (HP G1800 C) with

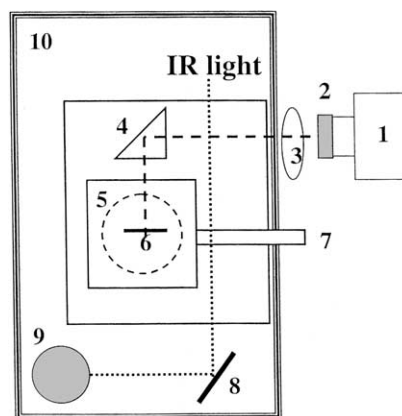


Fig. 2. Optical path for FT-IR measurements and broadband irradiation of BaY zeolite; 1. mercury lamp, 2. water filter, 3. broadband filter, 4. quartz prism, 5. FT-IR cell, 6. tungsten grid w/zeolite powder, 7. linear translator, 8. focusing mirror, 9. MCT detector, 10. FT-IR spectrometer (dry air purge).

a HP-5MS column (cross linked 5% PH ME siloxane). When available, standards of the products were injected separately to determine retention times and GC response factors.

3. Results

3.1. Photooxidation of cyclohexane using molecular oxygen

Initially, an adsorption isotherm was obtained for cyclohexane adsorption in BaY. Fig. 3 shows the FT-IR spectra of cyclohexane adsorbed in BaY as a function of cyclohexane pressure. The band at 1451 cm⁻¹ is assigned to –CH₂– and increases in intensity as the pressure of cyclohexane increases. The integrated area of this band was used to quantify the uptake of cyclohexane in the zeolite as shown in the inset of Fig. 3. The amount of cyclohexane was calibrated using volumetric methods. The difference in expansion pressure of cyclohexane with and without BaY present in the IR cell was determined at the highest pressures measured. From the calibrated volumes of the infrared cell and gas handling system, Δp , the pressure difference, was converted to the number of cyclohexane molecules absorbed in a sample of BaY. From the weight of the BaY sample,

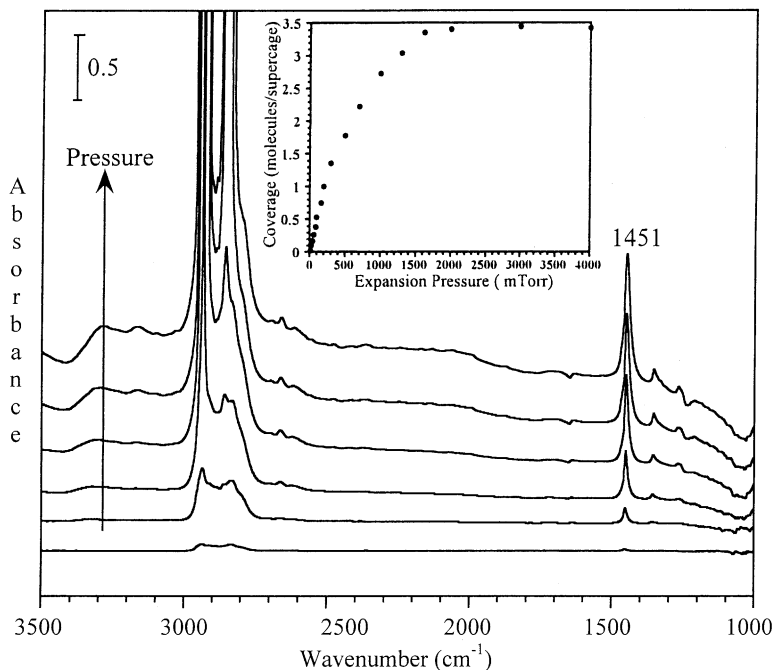


Fig. 3. FT-IR spectra of cyclohexane adsorbed in BaY as a function of cyclohexane pressure at $T = 298$ K. The absorption band at 1451 cm^{-1} was used to calibrate the uptake of cyclohexane as a function of pressure into the cell. The calibration was done using volumetric methods, see text for further details.

the number of supercages for that sample was determined as well. The integrated absorbance of the band at 1451 cm^{-1} at high pressure was then equated to the number of cyclohexane molecules per supercage determined above. Assuming that the band at 1451 cm^{-1} is linearly proportional to the number of cyclohexane molecules adsorbed in the zeolite, the number of cyclohexane molecules adsorbed per supercage could be determined at lower pressures as well. It can be seen in Fig. 3, that a coverage of 1 molecule cyclohexane per supercage is obtained at an equilibrium pressure of 200 mTorr. At a pressure above 1500 mTorr, the coverage reached a maximum of approximately 3.5 molecules cyclohexane per supercage.

The photooxidation of cyclohexane in BaY with O_2 was investigated using FT-IR spectroscopy. Fig. 4 shows the difference FT-IR spectra obtained after irradiation of cyclohexane (100 mTorr, 0.5 molecules cyclohexane per supercage) and O_2 in BaY at wavelengths greater than 455 nm. After broadband irradiation with $\lambda > 455\text{ nm}$, absorption bands at 1672

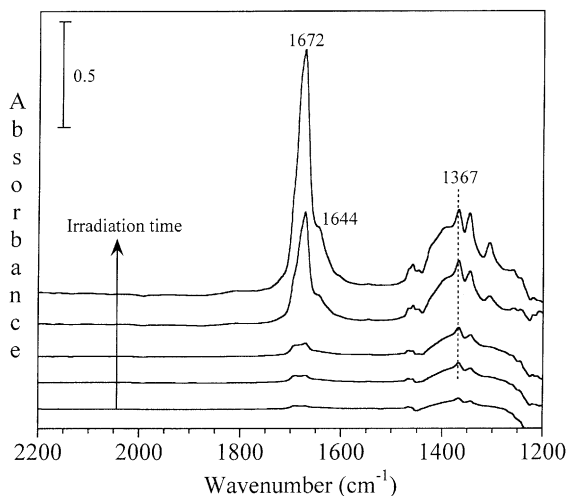


Fig. 4. Difference FT-IR spectra after irradiation of cyclohexane and oxygen in BaY with $\lambda > 455\text{ nm}$ near room temperature for 20 min, 1, 2, 6 and 22 h (bottom to top). Cyclohexane coverage in BaY was approximately 0.5 molecules per supercage.

and 1367 cm^{-1} are apparent in the spectrum. These indicate that cyclohexanone and cyclohexyl hydroperoxide, respectively, were produced [9]. The percent conversion of cyclohexane was calculated by measuring the decrease in the integrated area of the cyclohexane absorption at 1451 cm^{-1} (not observed in difference spectra) as the reaction occurs. The percent conversion after irradiation at $\lambda > 455\text{ nm}$ is determined to be 7%. Irradiation using a shorter wavelength filter, $\lambda > 325\text{ nm}$, gave a larger percent conversion of 48%.

The product distribution was also analyzed after completion of the FT-IR experiments by extracting the products from the zeolite sample in acetonitrile. GC analysis of the extracted products was then conducted to determine the product distributions that are presented in Table 1. The results indicate that $\sim 80\%$ of the products formed are cyclohexanone independent of the excitation wavelength. The other products formed are cyclohexanol (not observed in the FT-IR spectra [11,22]) and cyclohexyl hydroperoxide. Cyclohexyl hydroperoxide decomposes thermally to form cyclohexanone and water and may be the reason why it is not observed in GC analysis but is in FT-IR spectroscopy for experiments done at $\lambda > 455\text{ nm}$.

3.2. Photooxidation of cyclohexene using molecular oxygen

The FT-IR spectra of cyclohexene in BaY as function of cyclohexene pressure are shown in Fig. 5. The absorption band at 1636 cm^{-1} is assigned to the C=C stretching mode. This band was used to calibrate the uptake of cyclohexene in BaY as a function of expansion pressure (see inset of Fig. 5). A coverage of 1 molecule cyclohexene per supercage is seen to occur around 350 mTorr. Similar to that of cyclohexane,

the coverage leveled off at approximately 1 molecule cyclohexene per supercage at expansion pressures greater than $\sim 1500\text{ mTorr}$. For cyclohexene, the maximum coverage is determined to be 3 molecules per supercage.

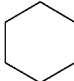
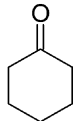
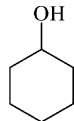
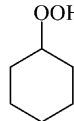
The photooxidation of cyclohexene with O_2 in BaY was monitored by FT-IR spectroscopy. The FT-IR difference spectra obtained after irradiation of cyclohexene (350 mTorr, 1 molecule cyclohexene per supercage) and O_2 in BaY at $\lambda > 455\text{ nm}$ are shown in Fig. 6. Several product bands attributed to C=O and C=C containing products are apparent in the $1600\text{--}1700\text{ cm}^{-1}$ region. The negative feature at 1440 cm^{-1} is due to loss of the reactant, cyclohexene. Similar difference spectra are observed when the sample is irradiated with photons of shorter wavelength, $\lambda > 325\text{ nm}$.

After the FT-IR experiment was completed, reactants and products were extracted from the zeolite in acetonitrile. Detailed product analysis of the resulting solutions was completed using GC and GC-MS methods. The product distributions obtained from the GC analysis are listed in Tables 2 and 3. For $\lambda > 325\text{ nm}$, the major product formed was 2-cyclohexen-1-one (35%). Smaller amounts of 2-cyclohexen-1-ol (7%) and hexanedial (23%) were also formed. The proposed pathways for the formation of the major products are shown in Scheme 2. Various “other” products were also formed and are listed in Table 3. The product distribution is not altered to any great extent with excitation wavelength.

3.3. Oxidation of cyclohexane and cyclohexene using TBHP

TBHP is a major industrial oxidant for the transformation of small olefins to epoxides. Recently,

Table 1
Product distribution (%) and conversion (%) for the photooxidation of cyclohexane in BaY

	$\xrightarrow{\text{BaY}}$				Conversion (%) ^a
O_2 , 325 nm, 100 mTorr ^b , 18 h		81	11	8	48
O_2 , 455 nm, 100 mTorr ^b , 18 h		86	14	0	7

^a Conversion (%) was calculated by integrating the reactant peak in the FT-IR spectrum. Estimated error = $\pm 3\%$.

^b The 100 mTorr corresponds to a BaY loading of approximately 0.5 molecules cyclohexane per supercage.

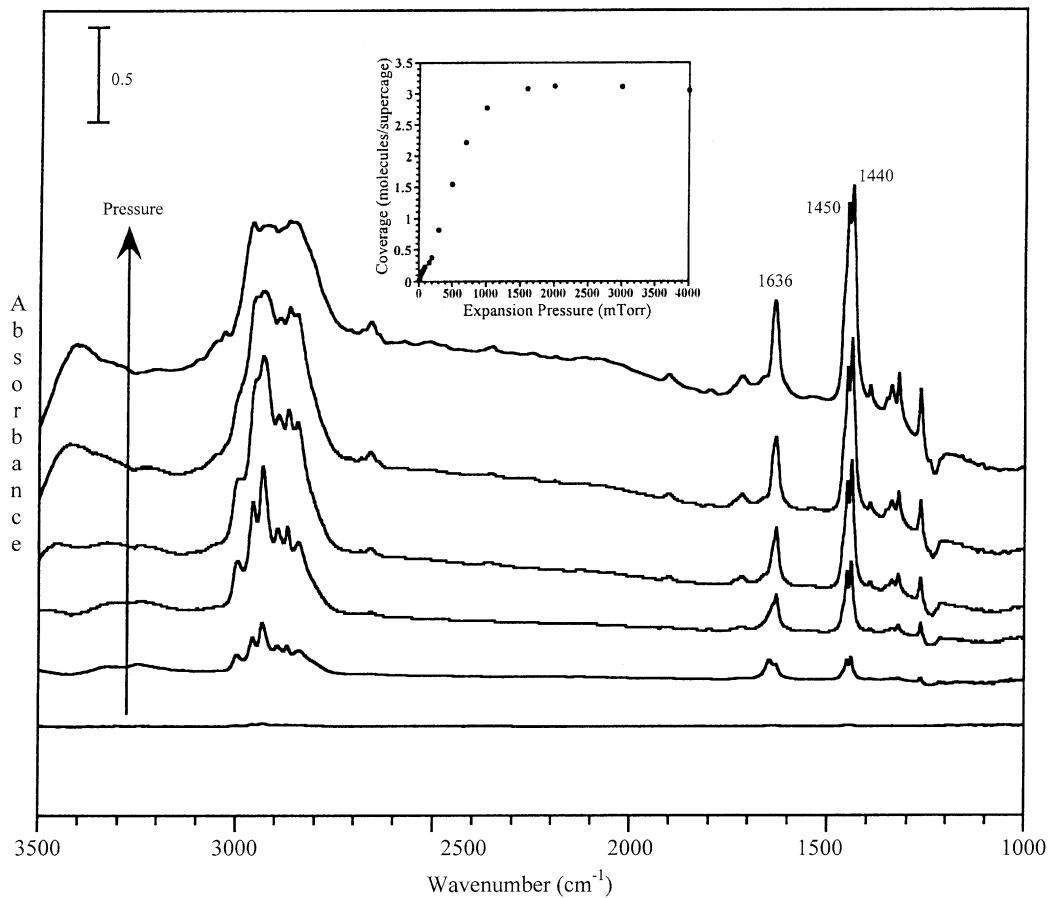


Fig. 5. FT-IR spectra of cyclohexene adsorbed in BaY as a function of cyclohexene pressure at $T = 298$ K. The absorption band at 1636 cm^{-1} was used to calibrate the uptake of cyclohexene as a function of pressure into the cell. The calibration was done using volumetric methods (see text for further details).

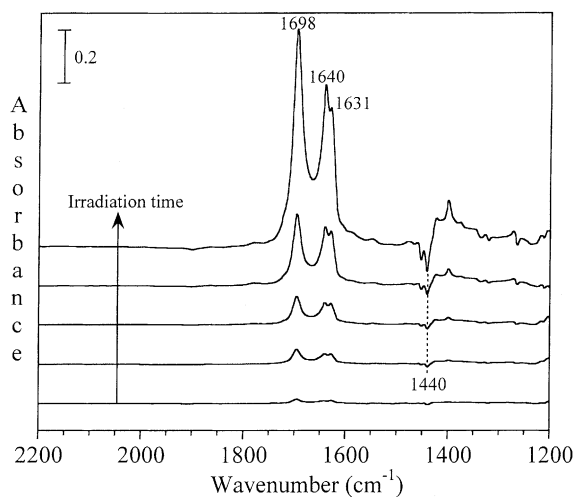
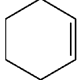
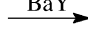
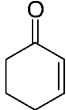
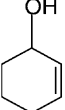
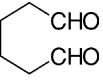
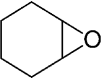


Fig. 6. Difference FT-IR spectra after irradiation of cyclohexene and oxygen in BaY with $\lambda > 455$ nm near room temperature for 20 min, 1, 2, 6 and 22 h (bottom to top). Cyclohexene coverage in BaY was approximately 1 molecule per surface site.

Table 2

Product distribution (%) and conversion (%) for the photooxidation of cyclohexene in BaY

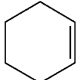
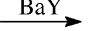
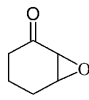
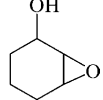
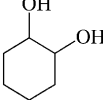
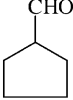
 					Other products	Conversion (%) ^a
O ₂ , 325 nm, 350 mTorr ^b , 23.5 h	35	7	23	0	35	64
O ₂ , 455 nm, 350 mTorr, 23.5 h	33	10	19	0	38	57
TBHP, thermal, 16 h	8	10	11	46	25	–

^a Conversion (%) was calculated by integrating the reactant peak in the FT-IR spectrum. Estimated error = ±3%.

^b The 350 mTorr corresponds to a BaY loading of approximately 1 molecule cyclohexene per superpage.

Table 3

Product distributions (percent of total products) for the other products from Table 2

 					Condensation product
O ₂ , 325 nm, 350 mTorr, 23.5 h	13	4	5	11	2
O ₂ , 455 nm, 350 mTorr, 23.5 h	11	4	11	6	5
TBHP, thermal, 16 h	4	2	1	9	9

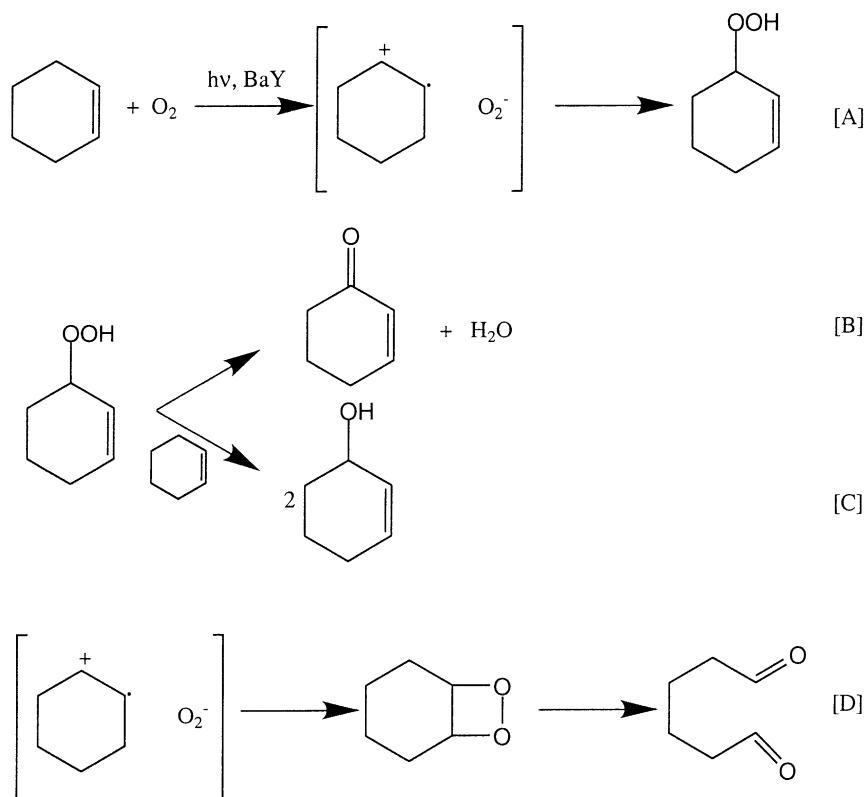
there have been several studies reporting the liquid phase epoxidation of cyclohexene in molecular sieves using TBHP [32–35]. In the experiments reported here, TBHP was generated in situ by irradiation ($\lambda > 400$ nm) of isobutane and molecular oxygen in BaY at 273 K [21]. The proposed mechanism for this reaction is shown in Scheme 3A and B. TBHP was then used to thermally oxidize cyclohexene (in the dark) (Scheme 3C). A competing, thermal reaction results in the formation of acetone and methanol from TBHP as shown in Scheme 3B [21]. The difference IR spectra of isobutane and oxygen in BaY before and after irradiation are shown in Fig. 7. The formation of TBHP (1377 cm^{-1}) and its thermal reaction product, acetone (1693 cm^{-1}), were observed. Frei and co-workers observed similar FT-IR spectra of isobutane and TBHP in BaY [21]. The FT-IR difference spectra obtained following the thermal oxidation of cyclohexene with TBHP in BaY as a function of time are shown in Fig. 8. The band at 1676 cm^{-1} indicates the formation of a C=O containing product. No reaction was observed when cyclohexene was added to BaY in the presence of TBHP.

After the FT-IR experiments were completed, the products and reactants were extracted from BaY in acetonitrile and the solutions were analyzed by GC and GC-MS. The product distributions determined by GC analysis are listed in Tables 2 and 3. The main product formed from the oxidation of cyclohexene with TBHP is 1,2-epoxy cyclohexane (46%) which is not seen in the FT-IR spectra because it has weak absorptions in the region where losses are seen for the reactant molecules. Smaller amounts of 2-cyclohexen-1-one (8%), 2-cyclohexen-1-ol (10%) and hexanedial (11%) are also formed as well as the other by-products listed in Table 3.

4. Discussion

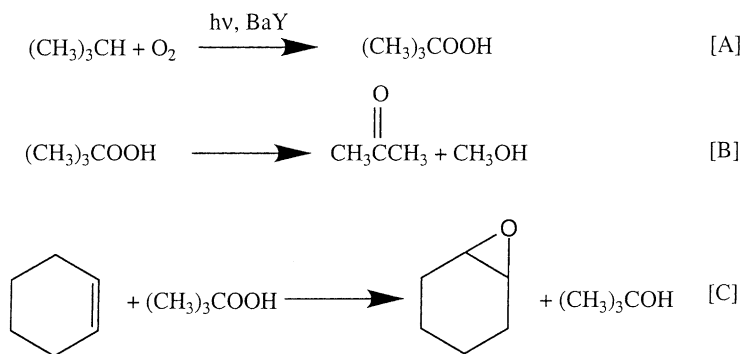
4.1. Influence of wavelength on product distribution

For cyclohexane, GC product analysis indicates that photooxidation with O₂ at different wavelengths results in similar product distributions. The cyclohexane

Scheme 2. Proposed mechanism for the photooxidation of cyclohexene with O_2 in BaY.

conversion measured by FT-IR spectroscopy increases from 7% at $\lambda > 455$ nm to 48% at $\lambda > 325$ nm. Based on these results, the conclusion is that better conversion of cyclohexane can be achieved at shorter wave-

lengths with no loss in selectivity. The wavelength dependence of the photooxidation of cyclohexene with O_2 is less dramatic. A slight increase in conversion is observed with wavelength; 64% at 325 nm



Scheme 3. Proposed mechanism for the oxidation of cyclohexene with TBHP in BaY.

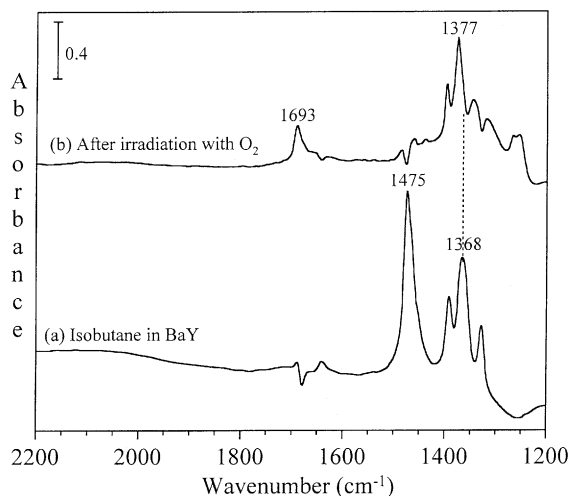


Fig. 7. (a) FT-IR spectrum of isobutane and oxygen adsorbed in BaY. (b) Difference FT-IR spectrum of isobutane and oxygen in BaY after irradiation with $\lambda > 455$ nm for 4 h.

relative to 57% at 455 nm. The product distribution does not change substantially. More hexanedial (23%) is formed at 325 nm relative to 455 nm (19%). This is consistent with previous work which showed that dioxetane chemistry was more prevalent at shorter irradiation wavelengths [26].

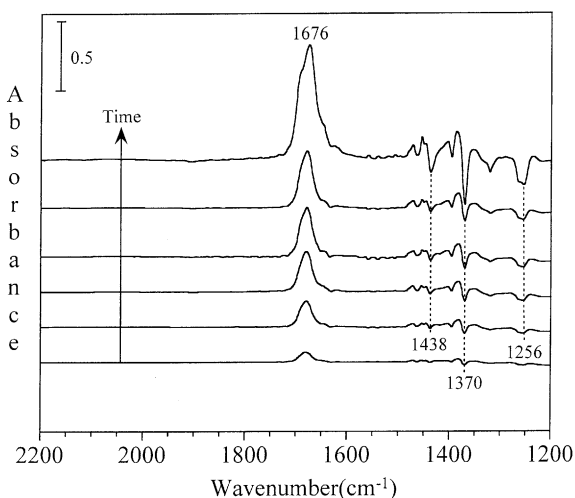


Fig. 8. Difference FT-IR spectra following the thermal oxidation of cyclohexene with TBHP generated in BaY for 20 min, 1–4 and 44 h (bottom to top).

4.2. Cyclohexane versus cyclohexene photooxidation in BaY

The photooxidation of cyclohexane in BaY with molecular oxygen yields cyclohexanone in approximately 80% product selectivity with smaller amounts of cyclohexanol ($\sim 10\%$) and cyclohexyl hydroperoxide ($\sim 0\text{--}10\%$). The proposed reaction routes for the formation of these products are given in Scheme 1. Cyclohexene photooxidation in BaY with molecular oxygen yields only $\sim 35\%$ of the analogous major product, 2-cyclohexen-1-one and 10% 2-cyclohexen-1-ol. Numerous other oxidation products, such as hexanedial ($\sim 20\%$) are also formed. Possible reaction paths for the formation of these three products in the photooxidation of cyclohexene are shown in Scheme 2. The first two reactions (A and B) are analogous to the cyclohexane chemistry shown in Scheme 1. The third reaction in Scheme 2 accounts for the formation of hexanedial through a dioxetane intermediate. Similar chemistry has been observed in related alkene photooxidation reactions in Y zeolites [4,20,26]. The other products listed in Table 3 are formed from secondary reactions of the products in Table 2. For example, 2,3-epoxycyclohexanone and 2,3-epoxycyclohexanol are formed from the epoxidation of 2-cyclohexen-1-one and 2-cyclohexen-1-ol, respectively.

These results indicate that cyclohexane photooxidation in BaY is more selective than cyclohexene photooxidation in BaY. The difference in observed selectivity can be attributed to the presence of two reactive centers ($\alpha\text{-H}$ and $\text{C}=\text{C}$ bond) in cyclohexene leading to multiple reaction paths as shown in Scheme 2. The percent conversion of cyclohexene (57%) after irradiation with $\lambda > 455$ nm is much greater than the percent conversion of cyclohexane (7%) under similar reaction conditions. The relative activity of H-abstraction by peroxide radicals from cyclohexene relative to cyclohexane is from 18 to 0.014 suggesting that cyclohexene should be much more reactive than cyclohexane [36] in these reactions.

4.3. Photooxidation of cyclohexene in BaY with different oxidants (O_2 versus TBHP)

TBHP was formed in situ in BaY from the photooxidation of isobutane with molecular oxygen as

shown in Scheme 3A. After removing excess isobutane and oxygen, cyclohexene was allowed to react thermally with TBHP in BaY. The main product formed from this reaction was 1,2-epoxy cyclohexane which accounted for 46% of the extracted products. Notably, no 1,2-epoxy cyclohexane was formed in the cyclohexene photooxidation reaction with molecular oxygen as the oxidant. The reaction pathway for the formation of 1,2-epoxy cyclohexane is shown in Scheme 3C. *tert*-Butanol is also formed stoichiometrically but was not detected by GC. Smaller amounts of 2-cyclohexen-1-one, 2-cyclohexen-1-ol and hexanedial were also formed after oxidation of cyclohexene with TBHP, as well as several other oxidation products listed in Tables 2 and 3. No reaction of cyclohexane and TBHP occurred under comparable reaction conditions. Presumably this is due to the fact that cyclohexane does not have a reactive double bond.

5. Conclusion

In the photooxidation of cyclohexane and cyclohexene in BaY using molecular oxygen, the main products formed were cyclohexanone and 2-cyclohexen-1-one, respectively. Cyclohexane photooxidation was found to be more selective than cyclohexene photooxidation in BaY with O₂ under comparable reaction conditions. The decrease in selectivity of cyclohexene relative to cyclohexane was attributed to the presence of two active reaction centers (α -H and C=C bond) in cyclohexene. The C=C functionality provided a route for dioxetane chemistry in cyclohexene that was not possible with cyclohexane as a reactant. Thermal oxidation of cyclohexene in BaY with TBHP changed the product distribution dramatically and resulted in the formation of 1,2-epoxy cyclohexane as the major product. No products were formed when cyclohexane was allowed to react with TBHP in BaY.

Future work includes further reaction studies in order to improve selectivity under mild reaction conditions and studies of the performance of different zeolites aimed at designing better oxidation systems. Additional exploration of product desorption from zeolites using a carrier gas and modestly elevated temperatures is important and nanocrystalline zeolites may be beneficial in this regard.

Acknowledgements

The authors want to thank Dr. Ping Li, Alexander Saladino and Jennifer Mann for valuable assistance with experiments. Although, the research described in this article has been funded wholly or in part by the Environmental Protection Agency through grant number EPA grant no. R829600 to SCL and VHG, it has not been subjected to the Agency's required peer and policy review and therefore does not necessarily reflect the views of the Agency and no official endorsement should be inferred.

References

- [1] F. Blatter, H. Sun, S. Vasenkov, H. Frei, *Catal. Today* 41 (1998) 297.
- [2] B.C. Gates, *Catalytic Chemistry*, Wiley, New York, 1992.
- [3] G.W. Parshall, S.D. Ittel, *Homogeneous Catalysis*, 2nd ed., Wiley, New York, 1992.
- [4] A.G. Panov, R.G. Larsen, N.I. Totah, S.C. Larsen, V.H. Grassian, *J. Phys. Chem. B* 104 (2000) 5706.
- [5] K.A. Suresh, M.M. Sharma, T. Sridhar, *Ind. Eng. Chem. Res.* 39 (2000) 3958.
- [6] I.W.C.E. Arends, R.A. Sheldon, M. Wallau, U. Schuchardt, *Angew. Chem. Int. Ed. Engl.* 36 (1997) 1144.
- [7] R. Raja, G. Sankar, J.M. Thomas, *J. Am. Chem. Soc.* 121 (1999) 11926.
- [8] J.D. Chen, R.A. Sheldon, *J. Catal.* 153 (1995) 1.
- [9] D.L. Vanoppen, D.E. Devos, M.J. Genet, P.G. Rouxhet, P.A. Jacobs, *Angew. Chem. Int. Ed. Engl.* (1995) 560.
- [10] G.X. Lu, H.X. Gao, J.H. Suo, S.B. Li, *J. Chem. Soc., Chem. Commun.* 21 (1994) 2423.
- [11] E.L. Pires, J.C. Magalhaes, U. Schuchardt, *Appl. Catal. A: Gen.* 203 (2000) 231.
- [12] H. Sun, F. Blatter, H. Frei, *J. Am. Chem. Soc.* 118 (1996) 6873.
- [13] X. Li, V. Ramamurthy, *J. Am. Chem. Soc.* 118 (1996) 10666.
- [14] D.L. Vanoppen, D.E. De Vos, P.A. Jacobs, *J. Catal.* 177 (1998) 22.
- [15] F. Blatter, H. Frei, *J. Am. Chem. Soc.* 115 (1993) 7501.
- [16] F. Blatter, H. Frei, *J. Am. Chem. Soc.* 116 (1994) 1812.
- [17] H. Sun, F. Blatter, H. Frei, *J. Am. Chem. Soc.* 116 (1994) 7951.
- [18] F. Blatter, F. Moreau, H. Frei, *J. Phys. Chem.* 98 (1994) 13403.
- [19] F. Blatter, H. Sun, H. Frei, *Catal. Lett.* 35 (1995) 1.
- [20] H. Frei, F. Blatter, H. Sun, *Chemtech* (1996) 24.
- [21] F. Blatter, H. Sun, H. Frei, *Chem. Eur. J.* 2 (1996) 385.
- [22] H. Sun, F. Blatter, H. Frei, *Catal. Lett.* 44 (1997) 247.
- [23] S. Vasenkov, H. Frei, *J. Phys. Chem. B* 101 (1997) 4539.
- [24] S. Vasenkov, H. Frei, *J. Phys. Chem. B* 102 (1998) 8177.
- [25] K.B. Myli, S.C. Larsen, V.H. Grassian, *Catal. Lett.* 48 (1997) 199.

- [26] Y. Xiang, S.C. Larsen, V.H. Grassian, *J. Am. Chem. Soc.* 121 (1999) 5063.
- [27] P. Li, Y. Xiang, V.H. Grassian, S.C. Larsen, *J. Phys. Chem. B* 103 (1999) 5058.
- [28] P. Carl, S.C. Larsen, *J. Catal.* 182 (1999) 208.
- [29] A.G. Panov, K.B. Myli, Y. Xiang, V.H. Grassian, S.C. Larsen, Photooxidation of toluene in cation-exchanged zeolites, in: P. Anastas, L.G. Heine, T.C. Williamson (Eds.), *Green Chemical Syntheses and Processes*, ACS, Washington, DC, 2000, p. 206.
- [30] R.G. Larsen, A.C. Saladino, T.A. Hunt, J.E. Mann, M. Xu, V.H. Grassian, S.C. Larsen, *J. Catal.* 204 (2001) 440.
- [31] T.M. Miller, V.H. Grassian, *J. Am. Chem. Soc.* 117 (1995) 10969.
- [32] M.S. Niassary, F. Farzaneh, M. Ghandi, L. Turkian, *J. Mol. Catal. A: Chem.* 157 (2000) 183.
- [33] Q.-H. Xia, X. Chen, T. Tatsumi, *J. Mol. Catal. A: Chem.* 176 (2001) 179.
- [34] M. Fujiwara, H. Wessell, P. Hyung-Suh, H.W. Roesky, *Tetrahedron* 58 (2002) 239.
- [35] J.P.M. Niederer, W.F. Holderich, *Appl. Catal. A: Gen.* 229 (2002) 51.
- [36] D. Nonhebel, J. Walton, *Free Radical Chemistry: Structure and Mechanism*, Cambridge University Press, Cambridge, 1974.